

SOIL THICKNESS SPATIAL DISTRIBUTION INFLUENCE ON FACTOR OF SAFETY EQUATION

Felipe Costa Abreu Lopes

Doutorando em Geografia e Professor do Instituto Federal de São Paulo, Jundiaí-SP¹
fcalopes@ifsp.edu.br

Irani dos Santos

Docente do Departamento de Geografia, Universidade Federal do Paraná, Curitiba-PR²
irani@ufpr.br

ABSTRACT: Mass movements occurrences are well studied, however there are still possible improvements regarding their factor of safety simulation. This paper focus on the influence of spatialized pedological data and geotechnical data, two of the major limitations for this type of modeling. Numerous mass movements were triggered by an extreme precipitation event in southern Brazil when the rainwaters reached 300mm in just 24 hours. A local watershed was chosen for field campaigns to supply a safety factor model and show the direct influence of field data on the result efficiency. For this, four different scenarios were created using combination of field data and spatialized soil thickness throughout the watershed area. The results showed an improve of 12% on the simulation efficiency when compared to a homogeneous soil thickness and average geotechnical values scenario, showing the importance of field studies for factor of safety simulations.

Key Words: spatially distributed soil thickness; slope stability; factor of safety.

INFLUÊNCIA DA DISTRIBUIÇÃO ESPACIAL DA ESPESSURA DO SOLO EM EQUAÇÃO DE FATOR DE SEGURANÇA

RESUMO: Movimentos de massa são muito estudados, porém há espaço para melhorias nas simulações de fator de segurança. Este artigo foca na influência da espacialização de dados pedológicos e dados geotécnicos, duas das principais limitações para esse tipo de modelagem. Inúmeros movimentos de massa aconteceram durante evento extremo no sul do Brasil, com alturas de precipitação atingindo 300 mm em apenas 24 horas. Uma bacia hidrográfica local foi escolhida para campanhas de campo e abastecer um modelo de fator de segurança para mostrar a influência direta dos dados de campo na eficiência dos resultados. Para isso, quatro cenários diferentes foram criados usando a combinação de dados de campo e a espessura do solo espacializada. Os resultados melhoram em 12% a eficiência da simulação quando comparados a um cenário de espessura do solo homogênea e valores geotécnicos médios, mostrando a importância dos estudos de campo para simulações de fatores de segurança.

Palavras-chave: espessura do solo distribuída espacialmente; estabilidade da encosta; fator de segurança.

INFLUENCIA DE LA DISTRIBUCIÓN ESPACIAL DEL ESPESOR DEL SUELO EN LA ECUACIÓN DEL FACTOR DE SEGURIDAD

RESUMEN: Los movimientos de masas se estudian ampliamente, pero se pueden hacer mejoras al simular su factor de seguridad. Este artículo se centra en la influencia de la espacialización de datos pedológicos y geotécnicos, dos de las principales limitaciones para este tipo de modelado. Incontables movimientos de masas tuvieron lugar durante un evento extremo en el sur de Brasil, con alturas de precipitación que alcanzaron los 300 mm en solo 24 horas. Se eligió una cuenca hidrográfica para las campañas de campo y para proporcionar un modelo de factor de seguridad que muestre la influencia directa de los datos de campo en la eficiencia de los resultados. Para esto, se crearon cuatro escenarios diferentes utilizando la combinación de datos de campo y el espesor del suelo espacializado. Los resultados mejoran la eficiencia de la simulación en un 12% en comparación con un escenario de espesor de suelo homogéneo y valores geotécnicos promedio, lo que demuestra la importancia de los estudios de campo para simulaciones de factores de seguridad.

Palabras clave: espesor del suelo distribuido espacialmente, estabilidad de taludes, factor de seguridad.

¹ Endereço para correspondência: IFSP - Avenida Dr. Cavalcanti, 396, Centro, CEP: 13201-003, Jundiaí-SP.

² Endereço para correspondência: UFPR - Avenida Cel. Francisco H. dos Santos, 100, Jardim das Américas, CEP: 81530-000, Curitiba-PR.

Introduction

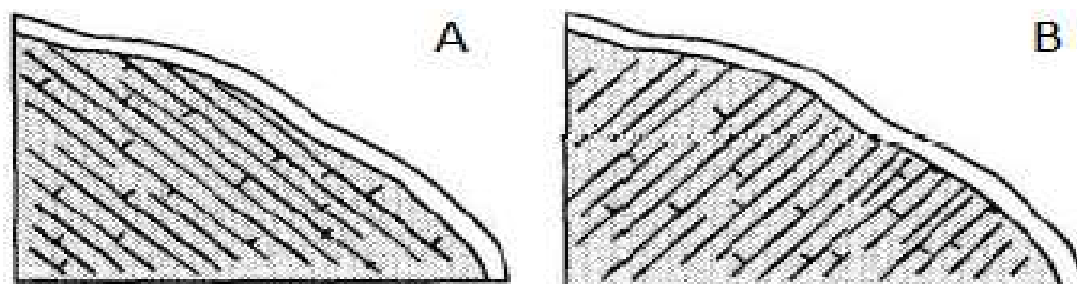
Mass movements are a great concern from small villages to big cities and their impacts are well known. Safaei et al (2011) point out that in the 20th century more than 500,000 people were affected by them in mountainous areas of developing countries. For this reason, the research about these mass movements have increased significantly in the first years of the 21st century (WESTEN; ASCJ; SOETERS, 2006) and still grow, with important application in Brazil due to the uncontrolled urban expansion observed in many cities, where mass movement prone areas are often occupied by the most vulnerable population. In the state of Rio de Janeiro, according to the UN, in 2011 there were more than 900 deaths and losses of up to 1.2 billion dollars due to landslides caused by heavy rains. Other Brazilian states also face the same problems every rain season, according to Rocha (2004), only in the state of Minas Gerais, between 1996 and 2004, 650 landslides were registered.

The classifications of different types of mass movements have been made since the beginning of the 20th century (NEMČOK; PAŠEK; RYBÁŘ, 1972). According to Safaei et al (2011) since the beginning of the 90s of the last century, several deterministic models have been created with the objective of pointing out areas susceptible to triggering landslides (SHASTAB, Montgomery; Dietrich, 1994; DSLAM, Wu; Sidle, 1995; SINMAP, Pack; Tarboton; Goodwin, 1998; among others). Each using different mathematical equations, which consider different variables to establish unstable areas by a factor of safety (FS).

Mass movements can theoretically occur anywhere on the planet. Not only steep slopes places are prone to material displacement, but also flatter areas can present such movements, like slow speed creeps. Large volumes of water (from rain, floods or other sources), seismic forces, volcanic and anthropogenic activities combined with external influences like precipitation, insolation, wind force and anthropic actions can trigger mass movement. Particularly in Brazil, more precisely in the group of ridges in south and southeast regions, the delicate slope stability balance acquired during their evolution in time is supported by some factors that affect the occurrence of mass movements, such as lithology, geomorphology, vegetation, moisture and soil characteristics.

The influence of lithological properties on mass movements is well discussed in the literature. According to Sidle; Pearce; O'loughlin (1985) rock properties are important factors in the balance of a slope. Weak rocks are linked to unfavorable geological structures to maintain this balance and give rise to environments with a large presence of mass movements. The presence of fractures, joints and lamination favors the accumulation of water and the consequent pressure increase in these rocks, which contributes to their weathering and greater fragility. Chatwin et al (1994) also discuss the orientation of bedding surfaces. When these are parallel to the topography, stability tends to be lower than when they are perpendicular (Figure - 1)

Figure 1 – Illustration of bedding surfaces. On the left are shown parallel bedding surfaces and on the right perpendicular bedding surfaces



Chatwin et al (1994).

The morphology of a slope can influence the triggering of a mass movement in several ways. The shapes of the slopes (plan and profile curvature) play an important role in the distribution and movement of water both on the surface and underground. Sidle; Pearce; O'loughlin (1985), Fernandes et al (2004) and Vieira (2007) point out that concave shapes favor the concentration of water and sediments while convex shapes favor the flow divergence. A higher surface and underground water concentration tends to create unstable areas on the slope. Although concavities favor the concentration of flow, in convex curvatures material displacement also happens because of the level of soil saturation and other natural factors.

The aspect informs the direction of the slope face, which gives information about how the slope is exposed to climatic factors such as, rain, and insolation. The greater exposure of the slope to these elements can influence the plant composition of the area and the thermal amplitude of the soils and moisture, which can help triggering mass movements. While aspect has a role on slope stability, research from last century to actual days show that its importance is not capital (BEATY (1956), DAI; LEE (2002), CLERICI et al (2006), MASOUMI; JAMALI; MOSTAFA (2014), CAPITANI; RIBOLINI; BINI (2013), METEN; PRAKASH BHANDARY; YATABE (2015) and HAMZA.; RAGHUVANSHI (2017).

Slope is another important factor in slope stability. The steeper the terrain, the more suitable for mass movements. Chatwin et al (1994) show that different slopes give origin to different types of mass movements from debris flows to rock falls. Highland; Bobrowsky (2008) point to a slope gradient from 20 degrees for the occurrence of translational landslides on slopes on United States. De Rose (2012) states that in the Te Whanga region (North Island, New Zealand) 95% of landslides are at a slope angle greater than 24 degrees. Fernandes et al (2004) cites studies carried out in Brazil that point to limiting angles for the occurrence of landslides between 20 and 29 degrees. As an important indicator of slope stability, slope is widely used as one of the slope stability modeling variables (Fernandes et al, 2004).

Moisture is another very important factor for slope stability influencing physically and chemically in the weathering, soil formation, relief erosion and in the distribution and typification of vegetation, (CHATWIN et al, 1994). The presence of water in the soil prior to rain events and its influence on the generation of runoff has been studied since Horton (1933). Since then, some models have proposed to simulate this antecedent moisture and its evolution in time and space (BEVEN; KIRKBY, 1979, TROCH; DE TROCH, 1993, BAUM; SAVAGE; GODT, 2002).

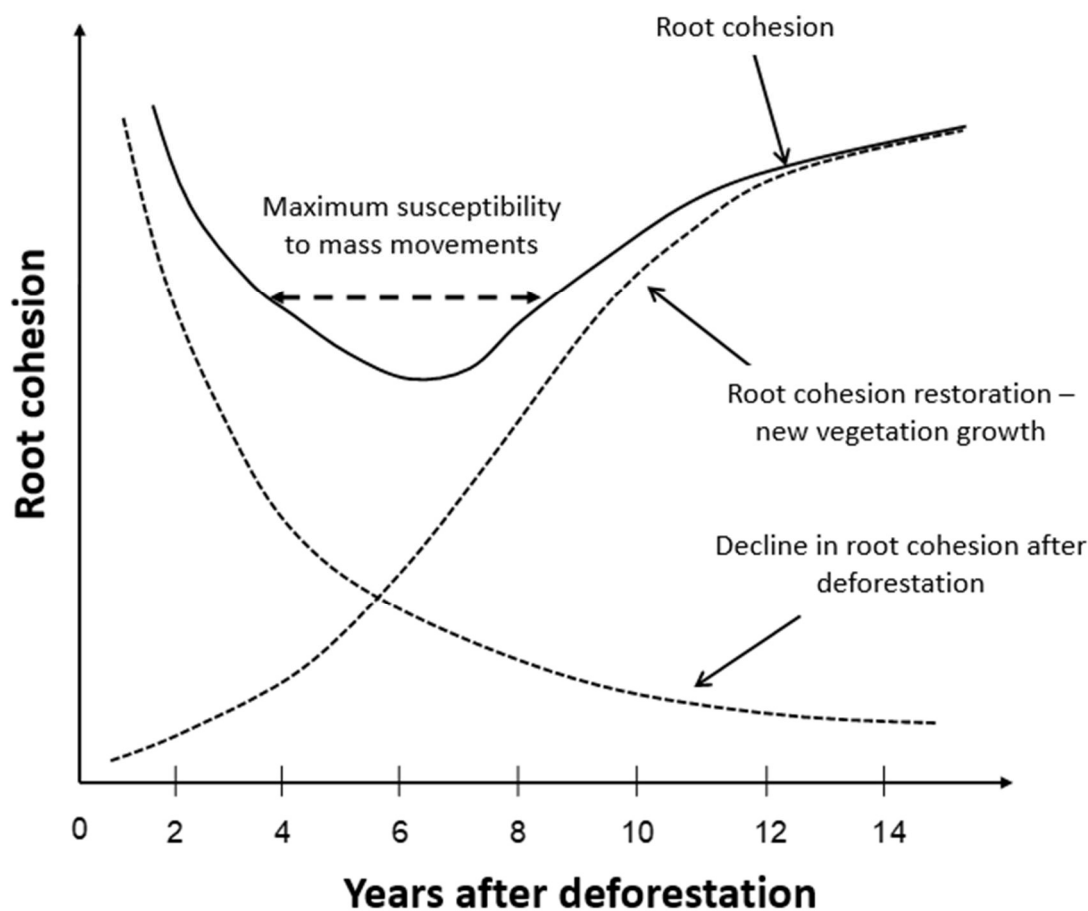
The variation of water table level is probably one of the most important factors in triggering a landslide. Soil saturation is one of the most common reasons for instability and its origin can be precipitation, melting or flooding (HIGHLAND; BOBROWSKY, 2008). The moisture directly reflects on the pressure it exerts on the pores and on the stability of a slope (SIDLE; PEARCE; O'LOUGHLIN, 1985). The pore-pressure exerted by water is directly proportional to the height of the water column present in this soil. In this case, in places where the soil already contains considerable moisture (from previous events), an extreme precipitation event is not needed for increasing the neutral pore-pressure and its influence on the stability of the slope.

According to Vieira (2007) studies on the influence of vegetation on slope stability began to be carried out in the beginning of the 20th century. Vegetation influences on slope stability can be positive and negative. They can favor stability by "anchoring" the soil with its roots, exerting root cohesion (BUENO et al, 2011 and CHATWIN et al, 1994). This type of cohesion has a small value compared to the soil cohesion strength, but as shown by Casadei; Dietrich; Miller, 2002 and Schwarz; Cohen; Or, 2010, it can influence on the slope stability. The root system is of greater importance in lithic neosoils, where these roots enter the rock fractures, and thus are more efficient in soil stability, on the other hand in deeper soils the fault plane can occur below the root zone, totally nullifying its influence. Above ground, vegetation

prevents direct soil erosion by rainfall through interception, thus minimizing the splash effect and surface runoff.

In the case of deforestation, Sidle; Pearce; O'loughlin (1985) state that the decay of the root system over time generates preferential paths and reduces the original cohesion of the roots, which contributes to the destabilization of the land a few years after deforestation (Figure - 2).

Figure 2 – Influence of roots on the maintenance of slope stability



Source: Sidle; Ochai (2000).

The presence of vegetation can also negatively influence the slope stability because of their weight, which on steep slopes is harmful, as well as they can act as a lever when strong winds hit the treetops (TABALIIPA; FIORI, 2008).

Among the deterministic models input data, soil data has many uncertainties, due to either the small amount of information, the objectives of the researchers or the limitation of how they were obtained (MCKENZIE; GALLANT; GREGORY, 2003). That is why they are generally used as secondary data or estimated according to the type of soil and its position on the landscape. Despite this, they have great importance in the slope stability, directly influencing it according to its thickness, cohesion, internal friction angle and specific weight. In addition, soils also store rainwater making slope stability susceptible to the moisture variation.

Chemical and physical structures of the soils, as well as its thickness are of great importance for mass movements research. The chemical structure of the soil, for example, in the presence of certain clay minerals, can be detrimental to the slope stability, since these clay

minerals have the capacity to store water between their blades (SIDLE; PEARCE; O'LOUGHLIN, 1985). The physical characteristics of soils represented by their texture and structure, directly influence cohesion, permeability, water table level and pore pressure, affecting their stability (IVERSON, 2000, CASADEI; DIETRICH; MILLER, 2003). Wang; Sassa (2003) affirm that finer soil grains, under a rain simulation experiment, developed superior pore-pressures and different landslide characteristics than in coarse grained soil (landslide movement presents higher speeds and rupture appears earlier). Soil saturated hydraulic conductivity (Ks) also have been used in research that correlate its change in soil profile with mass movements depth occurrence (VIEIRA; FERNANDES, 2004; VIEIRA, 2001; PELLETIER et al, 1997).

According to Sidle; Pearce; O'loughlin (1985), the smaller the soil thickness, the more propitious it will be to movements (due to the rapid saturation) and Acharya; Cochrane (2008) linked the soil thickness with the occurrence of landslides proving such a relationship with controlled laboratory experiments. The thickness of a soil is directly linked to its capacity of water storage and, therefore, its stability during precipitation events, however its determination depends on the objective of each research and data on soil thicknesses are scarce due to the difficulty of obtaining samples.

Remondo et al (2003) put the lack of accuracy in soil thickness data as well as its structure and composition as the main problems for their use on modeling landslides. Despite of it, some works show the importance of these properties and their variation in space. Ho et al (2012) showed that the spatial distribution of soil thickness decreased the overestimated areas of models for shallow translational landslides simulations, which is a common problem in this type of modeling.

Acharya; Cochrane (2008) carried out a laboratory experiment with soil ramps with four different thicknesses of sandy soil, and after simulating a 50 mm / h rain, they concluded that the deeper the soil the greater the amount and time of rain needed to trigger a landslide. D'odorico; Fagherazzi (2003) showed the importance of colluvium thickness in a hollow in relation to its stability, stating that if the slope is greater than the angle of friction of the colluvium, the thickness is proportional to its instability.

In order to improve the role of soil on the slope instability, this work highlight the influence of soil thickness and its moisture on the slope instability. The soil is taken as the regolith and its thickness was spatially distributed according to Mckenzie; Gallant; Gregory (2003). Different values of water table were simulated using rainfall and geotechnical field data to create instability scenarios with the application of a FS equation.

The study area is called Bom Brinquedo watershed. It is a first-order watershed located in the city of Antonina, Paraná state (Figure - 3). It has a total area of approximately 0.17 km², an altimetric variation of 152 meters and a slope angle ranging between 0 and 54.5 degrees. In March 2011, an extreme rain event occurred with daily rainfall greater than 300 mm in 24 hours. It was preceded by ten days with less intense and continuous rain and triggered several mass movements in the Serra do Mar region, with damage to roads, urban and rural infrastructure, in addition to loss of human lives (INPE, 2011).

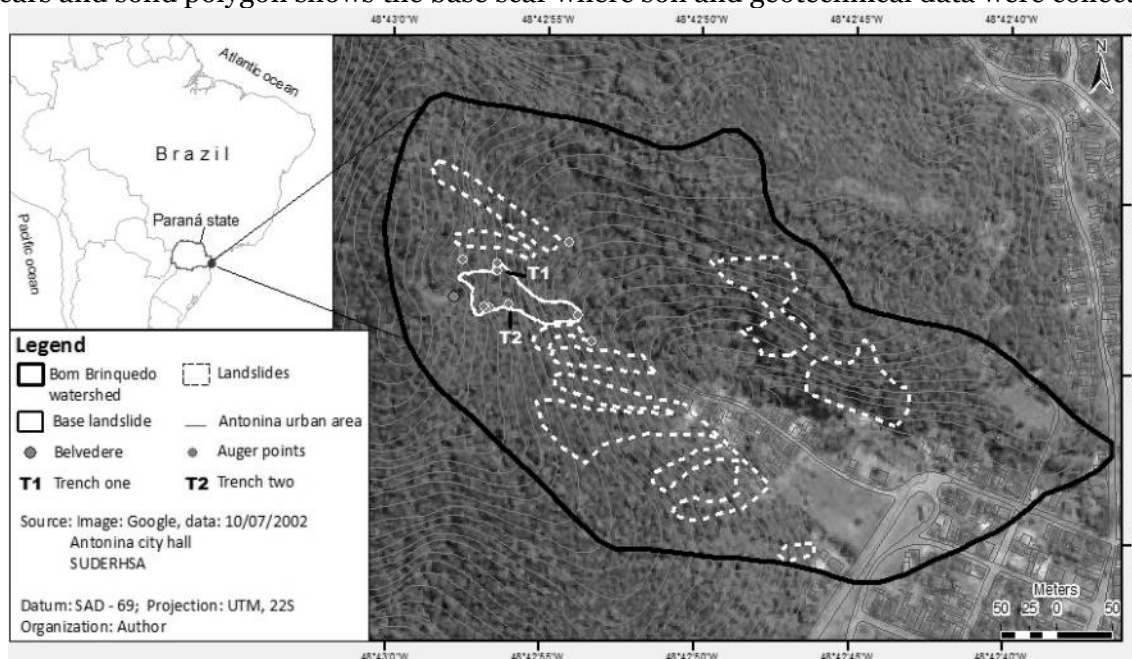
The land use of the watershed is predominantly tropical forest (82.3%) on its slopes, while in the valley houses with cobbled streets were found (representing 17.7% of the total area). Most of the houses were destroyed by the debris flow from the landslides.

The scars derived from the mass movements in the area were mapped with aerial images obtained by helicopter flights and from Google Earth data. One scar was chosen as the base scar (considering its size and accessibility) to carry out field work, soil sample collections for the geotechnical tests and for the determination of the soil thickness.,

The area is geologically part of the Paraná shield, consisting of rocks whose ages vary from the Archean (2.6 billion years) to the Lower Paleozoic (450 million years). The shield is partially covered by unconsolidated Cenozoic continental and marine sediments (MINEROPAR, 2001).

The climate fits Köppen's classification as cfa (Vanhoni and Mendonça, 2008). The rainfall in the coastal plain has its maximum in the summer months and average annual rainfall of approximately 2000 mm.

Figure 3 – Study area of Bom Brinquedo watershed. Dashed polygons show mass movements scars and solid polygon shows the base scar where soil and geotechnical data were collected



Methods

Topographic data and scar inventory

For the digital elevation model (DEM) built for this research, topographic information at a scale of 1: 10000 with five-meter equidistant level curves, control points and drainage network were obtained from the Antonina master plan dataset. The DEM was hydrologically consisted using the topogrid tool present in Arcgis 9.3 software. The scar inventory was prepared based on photographs and aerial footage of the study area provided by the NGO ADEMADAN and from Google Earth.

Soil thickness

Soil thickness data were obtained from nine auger surveys carried out around the base scar. They were made in order to reach the rock layer or any soil horizon with signs of altered rock and, thus, input them to the soil thickness distribution model. Two trenches were opened (one on each side of the base scar) to characterize the soil profile and collect undisturbed samples for direct shear tests and saturated hydraulic conductivity. The undisturbed samples for the direct shear tests were taken from the trenches in PVC cylinders measuring 20 centimeters in height by 15 in diameter. The collections were made at different depths, which were defined to represent the variation of the identified soil horizons. For the saturated hydraulic conductivity test, three smaller undisturbed samples were taken from the same locations and at the same depths with stainless steel cylinders measuring 5.3 centimeters high by 5.0 centimeters in diameter.

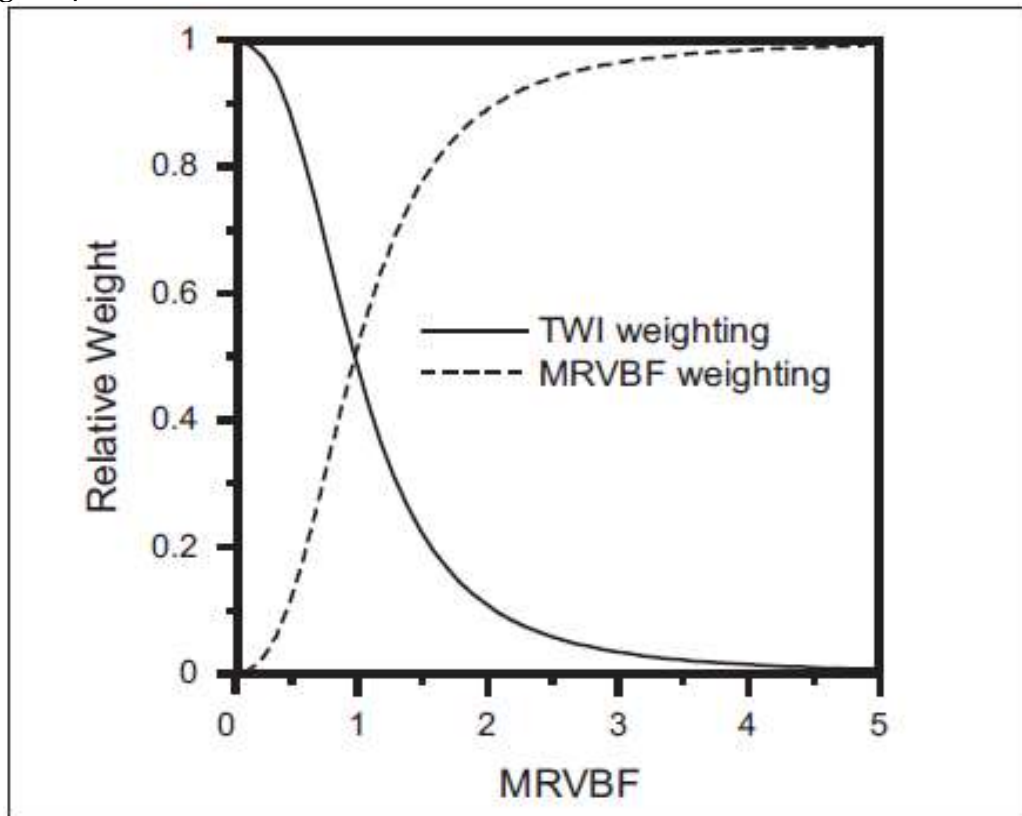
The spatial distribution of soil thickness was determined by the equation proposed by McKenzie; Gallant; Gregory (2003):

$$D = ITw * ITpred + MrVBFw * MrVBFpred \quad (1)$$

Where D is the soil thickness in meters, ITw is the wetness index weight, $ITpred$ is the predicted soil thickness in meters by the wetness index, $MrVBFw$ is the MrVBF (Multi-resolution valley bottom flatness index) weight and $MrVBFpred$ is the predicted soil thickness in meters by the MrVBF.

ITw presents higher values (equal or close to one) in steep slopes and/or divergent areas where there is a predominance of erosion, while in deposition areas $MrVBFw$ is more important and starts to have higher values. The transition areas are estimated using a form derived from the fuzzy logic illustrated in Figure - 4.

Figure 4 – Illustration of the relation between ITw and $MrVBFw$. $ITw + MrVBFw = 1$.



McKenzie; Gallant; Gregory (2003).

The topography index weight (ITw) is calculated by the equation:

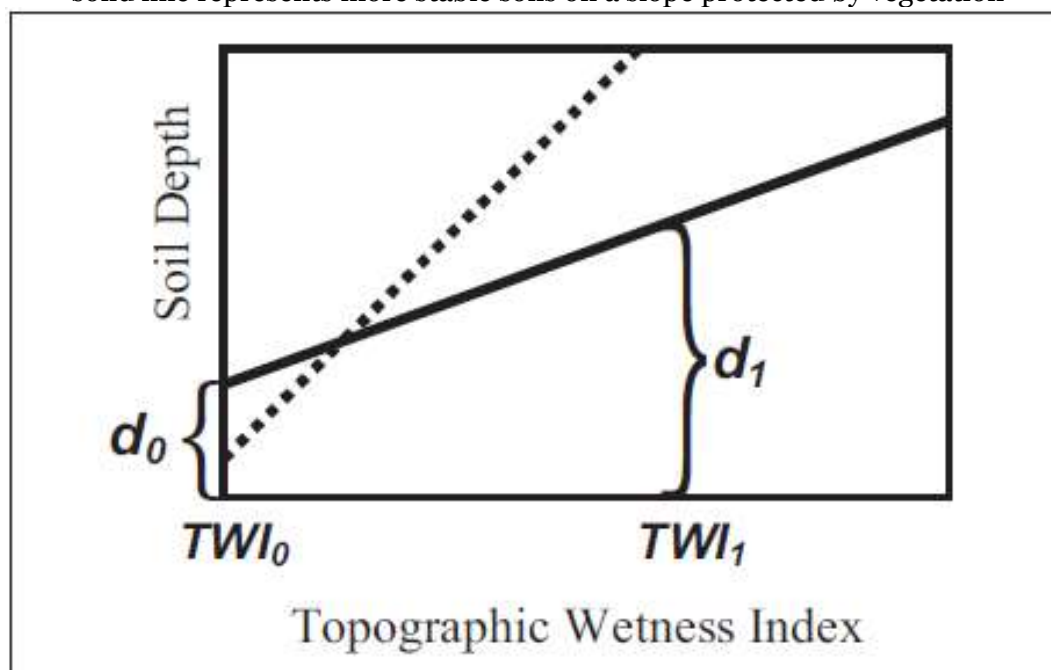
$$ITw = \frac{1}{1 + MrVBF^2} \quad (2)$$

Consequently, as the value of the topographic index and $MrVBFw$ weights add up to 1, the $MrVBFw$ weight is given by the equation:

$$MrVBFw = 1 - ITw \quad (3)$$

The IT_{pred} and $MRVBF_{pred}$ variables indicate the individually estimated soil thickness for the topographic index (IT) and MRVBF, respectively. The first is a preliminary soil thickness indicated only by the topographic index. Work by McKenzie; Ryan (1999) shows a linear relationship between topographic index and soil thickness (Figure – 5), thus it is used for the soil thickness spatialization. For the correct application of the Mckenzie; Gallant; Gregory (2003) an adaptation was necessary to fit the characteristics of the Bom Brinquedo watershed. In this research, MRVBF values greater than 1.5 indicates soil thickness (regolith) with minimum seven meters depth using a five-meter resolution DEM, instead of using the MRVBF value greater than 1.5 to areas with minimum five meters soil thickness (regolith) like the original methodology. These values are used for the determination of $MRVBF_{pred}$ variable.

Figure 5 – Linear relationship between topographic index and soil thickness in a slope. The dotted line represents more exposed soils on a slope that is directly affected by rain and the solid line represents more stable soils on a slope protected by vegetation



McKenzie; Gallant; Gregory (2003)

The IT_0 term means the topographic index value for the shallowest soil thickness value present in the soil inventory of the study site and IT_1 refers to the largest thickness value. McKenzie; Gallant; Gregory (2003) says that if the soil inventory is large enough, the 5th percentile of the soil thickness value can be used to represent IT_0 and the 50th percentile used to represent IT_1 . The data for the 5th and 50th percentiles of soil thickness for the Bom Brinquedo watershed were taken from values found in the augers and are respectively 4.0 and 4,7 meters. Teng et al (2008) present a formula to calculate the IT_{pred} variable for any topographic index value:

$$IT_{pred} = d_5 + \left(\frac{IT - IT_0}{IT_1 - IT_0} \right) * (d_{50} - d_5) \quad (4)$$

Where d_5 is the 5th percentile of soil thickness and d_{50} is the 50th percentile.

According to Murphy et al (2005) this methodology was applied to calculate soil thickness for watersheds in the region of New South Wales, Australia, where it had a good relationship with reality. Field validations showed that the model tends to overestimate its

results, but it is justified by the difficulty usually found in determining the thickness of soils, whether mechanical difficulties, inadequate instrument or research interest for only the first soil horizons.

Geotechnical data

Geotechnical tests to obtain cohesion, friction angle and specific weights of the soil were carried out at the Materials and Structures Laboratory (LAME) of the Institute of Technology for Development (LACTEC).

Direct shear tests were performed in accordance with ASTM D3080 / 1998 standards with nine undisturbed field collected soil samples from different soil horizons. Thickening pressures of 50, 100 and 200 kPa were exerted on them.

The saturated hydraulic conductivity (k_s) tests were performed at the Hydrogeomorphology Laboratory (LHG) of the Geography department at Universidade Federal do Paraná (Paraná Federal University - UFPR). The equation used to calculate saturated hydraulic conductivity (k_s) is as follows (LIBARDI, 2005):

$$k_s = \frac{aL}{A(\Delta t)} * \ln \frac{H1}{H2} \quad (5)$$

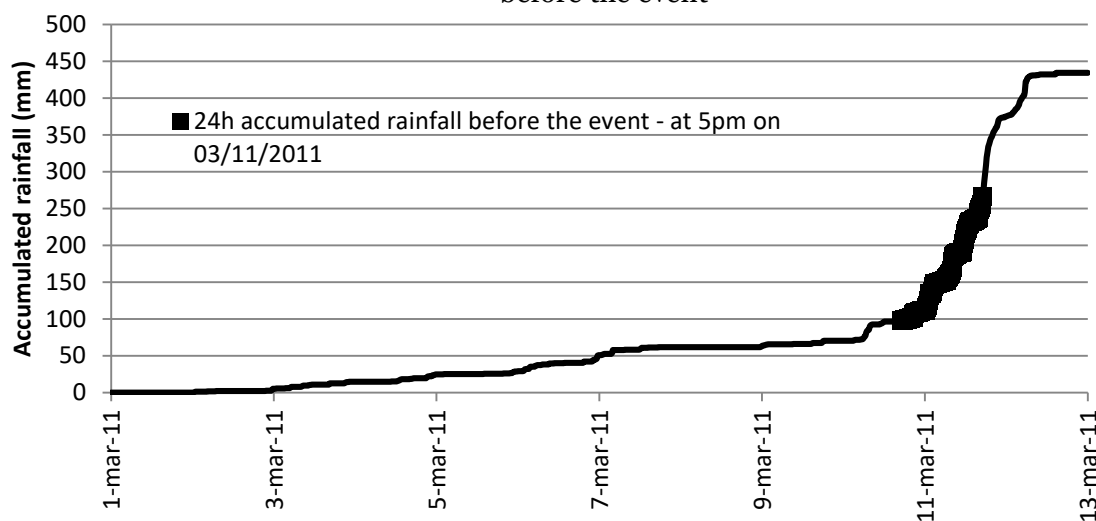
Where a is the cross-sectional area of the permeameter tube, L is the the soil sample length, A is the cross-sectional area of the soil sample, Δt is the time interval between measurements, $H1$ and $H2$ are, respectively, the initial and final water column reading heights.

The k_s together with the soil depth spatial distribution were used for the representation of the spatial distributed water table level in the Bom Brinquedo watershed according to the rain data.

Pluviometry data and water table level distribution

The selected pluviometry data were recorded every 15 minutes on the km35 meteorological station located 19 kilometers away from the study area. The month accumulated rainfall distribution until the time of the event (5 pm on March 11) can be seen below on Figure - 6.

Figure 6: accumulated rainfall distribution in March 2011 with the highlighted 24 hours before the event



During the day on which the mass movement occurred, the km35 meteorological station registered a rainfall greater than 200 mm, with a 24-hour accumulation prior to the landslide (from 5 pm on the 10th to 5 pm on the eleventh of March) of 169.6 mm against a total of 267.6 mm accumulated from the beginning of the month until the time of the event. This amount of rain in the previous 24 hours represents 63% of the total precipitated so far and 53% of the monthly average, which demonstrates the great concentration and the importance of this event for slope stability simulating research.

The water table level was calculated from the rainfall accumulated in 1, 6, 12 and 24 hours before the event using equation (6) (BEVEN; KIRKBY, 1979):

$$zl = \frac{s}{pt} \quad (6)$$

Where zl is the water table level (m), s is the moisture deficit (m) e pt is the total porosity (%).

Safety factor

The safety factor (SF) was obtained per pixel cell by Excel software calculations according to the equation (7) (FIORE; CARMINGANI, 2009):

$$FS = \frac{c + (h1 \gamma_{nat} + h2 \gamma_{sub}) \cos 2 \phi}{(h1 \gamma_{nat} + h2 \gamma_{sub} + h2 \gamma_a) \sin \phi \cos \phi} \quad (7)$$

Where c represents the cohesion (kPa), $h1$ is the dry soil length (m), $h2$ is the water table level (m), ϕ is the internal friction angle (degrees), γ_{nat} is the soil unit weight (kN/m³), γ_{sub} is the submerged soil unit weight (kN/m³) and γ_a is the water unit weight (kN/m³).

Different scenarios were elaborated to obtain different SF values to assess the influence of the soil thickness, its geotechnical properties and the water table level in the slopes of the Bom Brinquedo watershed.

Two main scenarios were created, each with four secondary scenarios and a third and last scenario was used as a basis for comparison. The first group of scenarios was called “geotechnical scenarios” (GS) and is characterized by the variation of geotechnical data: cohesion, internal friction angle and soil unit weights, according to the geotechnical tests for each soil horizons. In these scenarios, the water table level is kept fixed for the whole study area at its highest value based on the average k_s value for the soil horizons and the accumulated rainwater at the moment of the critical mass movement event (169 mm). The soil unit weights value vary according to the soil horizon, thus, in addition to being distributed, the total soil thickness varies for each scenario, since each soil horizon represents a scenario. By the equation (7), the dry unit weight and the saturated unit weight are multiplied, respectively, by the dry soil length ($h1$) and the water table level ($h2$). In this way, it is intended to identify which of the four soil horizons has a greater SF and efficiency (according to a confusion matrix) for the given moisture.

Table 1 – Geotechnical data used in GS scenarios. The soil unit weights are already multiplied by its respectively $h1$ and $h2$

Geotechnical Scenarios (GS)				
Scenario	Cohesion (kPa)	Internal friction angle (degree)	Dry unit weight (kN/m ³)	Saturated unit weight (kN/m ³)
GS1-169	10,95	27,7	7,6	11,7
GS2-169	15,25	24,56	11,4	15,5
GS3-169	4,35	29,34	13,9	20,4
GS4-169	0	34,14	16,5	21,2

The second group of scenarios, called water table level scenarios (WTL 1 to 4), aims to assess the influence of soil moisture on landslides occurrence. For this, the geotechnical data of the most efficient geotechnical scenario are fixed for the whole Bom Brinquedo watershed and the water table depth varies according to the equation (6).

In this way, four secondary scenarios are assembled with the water table level values calculated from the rainfall accumulated in 24, 12, 6 and 1 hours before the event (Table - 2).

Table 2 – Data used in water table scenarios (WTL)

Water table level (WTL) scenarios			
	Cohesion (kPa)	Internal friction angle (degree)	Precipitation (mm)
WTL 1			169
WTL 2	Geotechnical data from the most efficient		117
WTL 3	Geotechnical Scenario		76
WTL 4			29

The third and last scenario simulates the most common situation found in slope stability models, where the soil and the water table have homogeneous thickness and depth for the whole area. For this, the soil thickness was determined by the average of the values obtained in the field campaigns, the accumulated rainwater in 24 hours (169 mm) was used to determine the water table level and the geotechnical data of the GS4-169 scenario were used because they are the most pessimistic. This scenario aims to compare the results of the method of this research towards the generalizations that are made for the soil data (due to its difficulty of obtention).

The scenarios were validated according to the pixel classification as unstable and stable, interpreted as a binary classification. The efficiency of this result was measured with a simple confusion matrix, which predicts the success and the error for each of the two simulated classes when compared with the landslide scar inventory. Thus, the pixels indicated as both unstable and stable will be considered (Table - 3).

Table 3 - Binary confusion matrix scheme

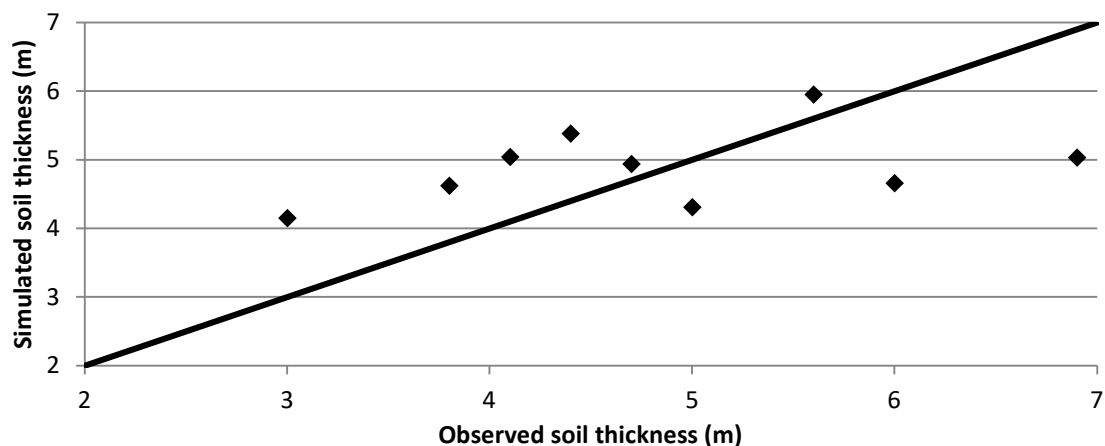
Class	Unstable Pixels	Stable Pixels	Class efficiency (CE)	Total efficiency (TE)
Unstable areas	True positive (tp1)	False negative (fn2)	$tp1/(tp1 + fn2)$	$(tp1 + tn2)/n$
Stable areas	False positive (fp1)	True negative (tn2)	$tn2/(tn2 + fp1)$	

Results

Soil thickness and pluviometry data

The soil thickness calculated pixel by pixel in the Excel software for the Bom Brinquedo watershed indicated a Directly Proportional relation with the soil thickness obtained in the field as shown in Figure - 7.

Figure 7 – relation between observed and simulated soil thickness



From the distributed soil thickness and the four accumulated Rainwater interval, different water table level, calculated according to equation (6), resulted in distinct proportions of saturated areas for the study area, as shown in table - 4.

Table 4 - Proportion of saturated and unsaturated areas for each accumulated Rainwater value

Accumulated Precipitation (mm)	Saturated area (%)
29	36,69
76	74,26
117	87,46
169	94,56

Scenario's efficiency simulation

The first group of scenarios sought the best simulation efficiency in slope stability according to the variation of geotechnical data in the study area, keeping the water table level constant based on a 169 mm accumulated rainwater 24 hours before the event triggering. For each scenario, the proportion of unstable areas are showed in table – 5 and its efficiency according to the confusion matrix is in the table – 6.

Table 5 - Unstable areas for each geotechnical scenario

Scenarios	Unstable areas (%)
GS1-169	19,11
GS2-169	20,99
GS3-169	33,44
GS4-169	30,83

Table 6 - Confusion matrix scheme for geotechnical scenarios

Scenarios	True positive	False positive	False negative	True negative	Total efficiency
GS1-169	13986	19001	129519	10131	0,831
GS2-169	14854	21383	127137	9263	0,822
GS3-169	19682	38043	110477	4435	0,754
GS4-169	18820	34399	114121	5297	0,770

The highest efficiency index was found in the GS1-169 scenario, coinciding with the lowest proportion value of unstable area also obtained by this scenario. This agrees with discussions found in the literature about the exaggeration of models used to simulate slope instability and with one of the objectives of this work, which seeks a better representativeness of the simulations in relation to mass movement scar inventories.

The group of scenarios with water level variation showed the influence of soil moisture for the simulation of slope stability. This group of scenarios consists of four scenarios, which make use of the most efficient geotechnical attributes from the GS scenarios, represented by the GS1-169 scenario. The variation of the water table level was calculated according to the rainwater for 1, 6, 12, and 24 hours prior to landslides, respectively 29 mm, 76 mm, 117 mm and 169 mm. As expected, the greater the amount of moisture, the greater the unstable area proportion in the study area (Table - 7). The efficiency according to the confusion matrix for the WTL scenarios is in the table – 8.

Table 7 – Proportion of unstable areas for the WTL scenarios

Scenarios	Precipitation (mm)	Unstable areas (%)	Saturated areas (%)
WTL-29	29	14,99	36,69
WTL-76	76	18,42	74,26
WTL-117	117	18,91	87,46
WTL-169	169	19,11	94,56

Table 8 - Confusion matrix scheme for WTL scenarios

Scenarios	True positive	False positive	False negative	True negative	Total efficiency
WTL-29	12103	13770	134750	12014	0,851
WTL-76	13863	17931	130589	10254	0,837
WTL-117	13980	18668	129852	10137	0,833
WTL-169	13986	19001	129519	10131	0,831

The highest efficiency index was found on WTL-29 scenario. The result shows that the smaller amount of moisture was enough to both start triggering the mass movements and decrease the overestimated simulated areas.

The uniform distribution scenario (Figure - 7) was simulated to show the influence of the spatial soil thickness distribution in the slope stability simulations. Therefore, it was conceived as an example of some consolidated models of slope stability, which consider a homogeneous soil thickness for the entire study area.

The water table was simulated with the 24-hour precipitation (169 mm) and the most pessimistic values were considered for the geotechnical parameters.

The efficiency according to the confusion matrix for the Uniform scenario is shown in the Table – 9.

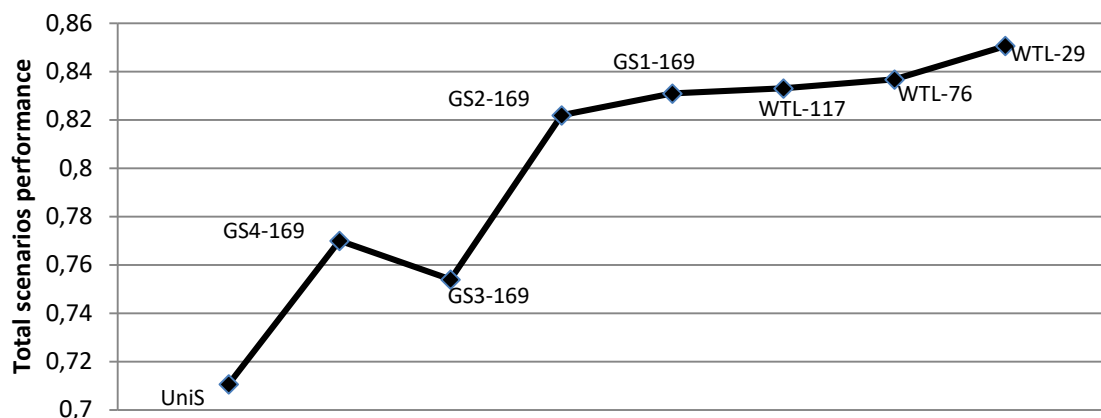
Table 9 – Confusion matrix scheme for Uniform scenario

Scenario	True positive	False positive	False negative	True negative	Total efficiency
UniS	21314	47143	101377	2803	0,711

Discussion and conclusions

The soil thickness spatial distribution together with the variation of the geotechnical data and water table level improved the performance of the simulations by 12% in relation to the uniform scenario (from 0.71 to 0.83 of total efficiency, Figure - 8).

Figure 8 - Comparison of the total performances of the simulated scenarios



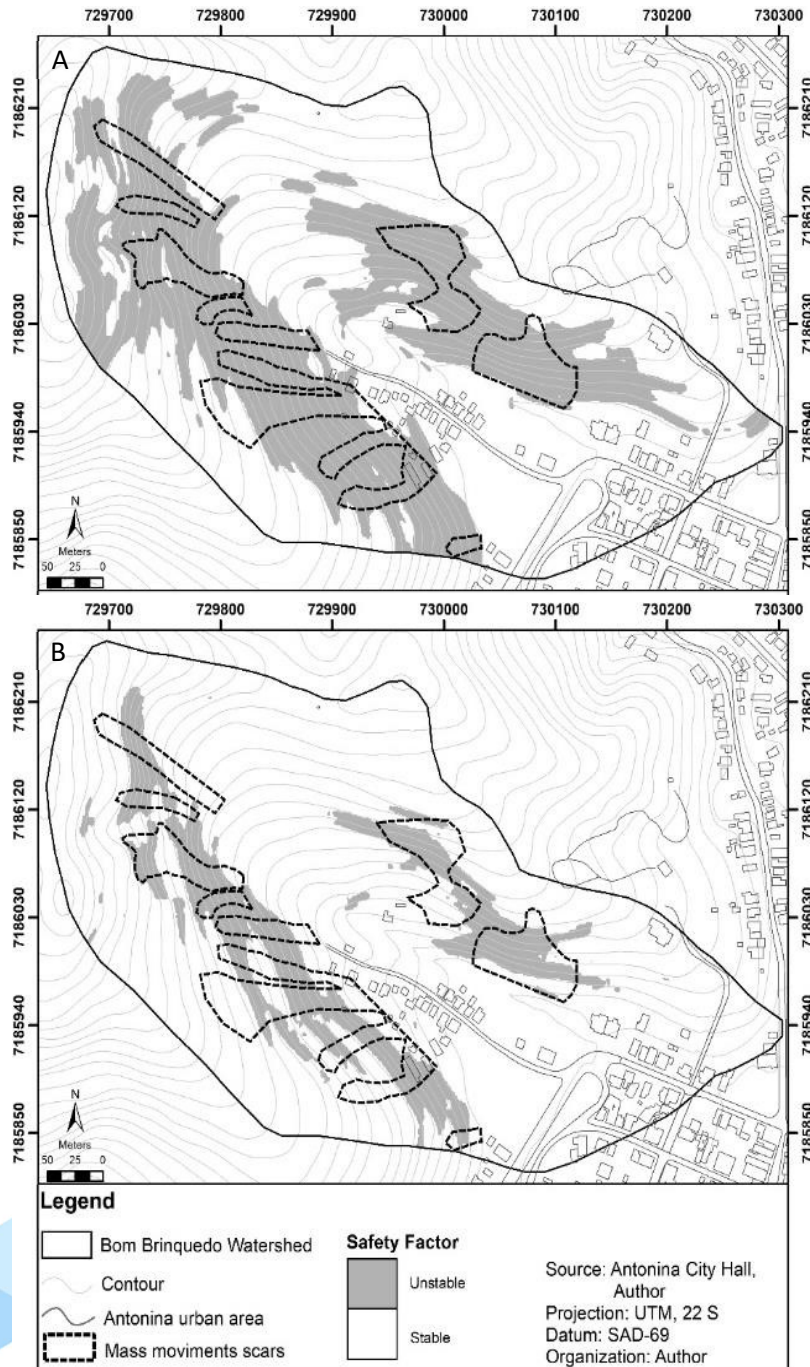
As shown in figure – 8, the variation of the water table level values had no significant sensitivity in the total simulation efficiency, since the lowest value was sufficient to saturate the areas where the mass movements occurred. Even so, an improvement in the result was verified with the variation of moisture. The Figure - 9 shows the Uniform and the WTL-29 scenarios.

The geotechnical scenarios showed a big improvement in the simulation efficiency specially from GS3-169 to GS2-169. This leap is explained mainly by the difference in the cohesion value between these two scenarios. Another significant observation is that the GS3-169 scenario is less efficient than the GS4-169, even if the last has a null cohesion value. The key factor here was the internal friction angle that is way higher in the GS4-169 scenario giving it a batter stability and efficiency. It highlights the discussion that not always the deepest soil horizon is the most unstable. In this case the fault plain occurred in the 3rd soil horizon.

The use of homogeneous data for the entire study area causes an exaggeration in the delimitation of the simulated unstable areas, reducing the efficiency of the simulation. In agreement with this conclusion, Ho et al (2012) stated that the distribution of soil thickness decreased the overestimation of unstable areas in the modeling of slope stability and thus increasing the efficiency of the model. Vieira (2007) pointed out that the variation of geotechnical data in different simulations with the SHALSTAB model also directly influenced their results. This shows the importance of the field data on simulation research and that a bigger effort must be made to improve the soil database, especially in the most vulnerable mass movement areas.

It was found that the variation of geotechnical data generates very different simulation efficiency, which shows the importance of knowing the range of these parameters variation to carry out more precise and less mistaken slope stability study. Although valuable, the geotechnical data are punctual and demand a lot of time for their collection, analysis and interpretation, showing that to have more efficient results for stability models, the studied site must have a continuous monitoring. This links the efficiency of the results directly to the monitoring data series.

Figure 9 – A: Uniform scenario: $c = 0 \text{ kPa}$, $\Phi = 34.4^\circ$, $\gamma_{\text{nat}} = 16.5 \text{ kN/m}^3$ e $\gamma_{\text{sat}} = 21.20 \text{ kN/m}^3$, average soil thickness = 4.2m and rainwater = 169 mm. B: WTL-29 scenario: $c = 10.95 \text{ kPa}$, $\Phi = 27.7^\circ$, $\gamma_{\text{nat}} = 7.6 \text{ kN/m}^3$ e $\gamma_{\text{sat}} = 11.7 \text{ kN/m}^3$, spatial distributed soil thickness and rainwater = 29 mm



Acknowledgements

This research was supported by CNPq (Brazilian National Research Council) and Universidade Federal do Paraná (Paraná Federal University).

References

- ACHARYA, G., COCHRANE, T.A. Rainfall Induced Shallow Landslides on Sandy Soil and Impacts on Sediment Discharge: A Flume Based Investigation. In: The 12th International Conference of International Association for Computer Methods and Advances in Geomechanics (IACMAG), Goa, India. 2008.
- BAUM, R.L., SAVAGE, W.Z., AND GODT, J.W. TRIGRS--A FORTRAN Program for Transient Rainfall Infiltration and Grid-Based Regional Slope-Stability Analysis. U.S. Geological Survey Open-File Report, 02-0424, p. 35, 2002.
- BEATY, C. B. Landslide and slope exposure. *Journal of Geology*. 64, p. 70 – 74, 1956.
- BEVEN, K. J. AND KIRKBY, M. J. A. Physically Based Variable Contributing Area Model Of Basin Hydrology. *Hydrol. Sci. Bull.* Vol. 24, p. 43-69, 1979.
- CAPITANI, M.; RIBOLINI, A.; BINI, M. The slope aspect: a predisposing factor for landsliding? *Comptes Rendus Geoscience*, 345, p.427-438, 2013.
- CASADEI, M., DIETRICH, W.E., MILLER, N L. Testing a Model For Predicting The Timing And Location Of Shallow Landslide Initiation In Soil-Mantled Landscapes. *Earth Surf. Process. Landforms*, 28, p. 925–950, 2003.
- CHATWIN, S.C., HOWES, D.E., SCHWAB, J.W., SWANSTON, D.N. A Guide for Management of Landslide-Prone Terrain in the Pacific Northwest. Research Branch, Ministry Of Forests, Victoria, British Columbia, Canada, 1994.
- CLERICI, A.; PEREGO, S.; TELLINI, C.; VESCOVI, P. A GIS-based automated procedure for landslide susceptibility mapping by the Conditional Analysis method: the Baganza valley case study (Italian Northern Apennines). *Environ Geol*, 50, p. 941-961, 2006.
- DAI, F. C.; LEE, C. F. Landslide characteristics and slope instability modeling using GIS, Lantau Island, Hong Kong. *Geomorphology*, 42, p. 213–228, 2002.
- DE ROSE, R. C. Slope control on the frequency distribution of shallow landslides and associated soil properties, North Island, New Zealand. *Earth Surface Processes and Landform*, 38, p. 356 – 371. 2012.
- D'ODORICO, P. FAGHERAZZI, S. A probabilistic model of rainfall-triggered shallow landslides in hollows: A long-term analysis. *Water Resour. Res.*, 39, p. 1262, 2003.
- FERNANDES, N.F., GUIMARÃES, R.F., GOMESA, R.A.T., VIEIRA, B.C., MONTGOMERY, D.R., GREENBERG, H. Topographic controls of landslides in Rio de Janeiro: field evidence and modeling. *Catena*, 55, p. 163–181, 2004.

FIORI A.P., CARMIGNANI L. Fundamentos de mecânica dos solos e das rochas: aplicações na estabilidade de taludes, second ed., Curitiba: UFPR, 2009.

HAMZA, T.; RAGHUVANSHI, T. K. GIS based landslide hazard evaluation and zonation – A case from Jeldu district, central Ethiopia. Journal of King Sand University, 29, p. 151-165, 2017.

HIGHLAND, L.M., AND BOBROWSKY, P. The landslide handbook—A guide to understanding landslides: Reston, Virginia, U.S. Geological Survey Circular 1325, 129 p. 2008

HO, J.Y., LEE, K.T., CHANG, T., WANG, Z., LIAO, Y., Influences of spatial distribution of soil thickness on shallow landslide prediction. Engineering Geology. 124, p. 38-46, 2012.

HORTON, R.E. The role of infiltration in the hydrologic cycle. Trans. Am. Geophys, vol. 14, p. 446-460, 1933.

INPE – INSTITUTO NACIONAL DE PESQUISAS ESPACIAIS, Análise de um evento de chuva intensa no litoral entre o PR e nordeste de SC. 2011. Disponível em <<http://www.cptec.inpe.br/noticias/noticia/16905>>

IVERSON, R.M., Landslide triggering by rain infiltration. Water resources research. 36, p. 1897–1910, 2000.

LIBARDI; P. L. Dinâmica da água no solo, São Paulo: Edusp, 2005.

MASOUMI, H.; JAMALI, A. A.; MOSTAFA, K. Investigation of role of slope, aspect and geological formations of landslide occurrence using statistical methods and gis in some watersheds in chahar mahal and bakhtiari province. Journal of Applied Environmental and Biological Sciences, 4, p. 121-129, 2014.

MCKENZIE, N.J., RYAN, P.J. Spatial prediction of soil properties using environmental correlation. Geoderma, vol. 89, p. 67-94. 1999.

MCKENZIE, N., GALLANT, J., GREGORY, L. Estimating water storage capacities in soil at catchment scales. Technical Report 03/3. Cooperative Research Centre for Catchment Hydrology, Canberra, Australia, 2003.

METEN, M.; PRAKASH BHANDARY, N.; YATABE, R. Effect of landslide factor combinations on the prediction accuracy of landslide susceptibility maps in the Blue Nile gorge of central Ethiopia. Geoenvironmental Disasters, 2, p. 1-17, 2015.

MINEROPAR, Atlas Geológico Do Estado Do Paraná, Curitiba: Mineraiis Do Paraná S/A, 2001.

MONTGOMERY, D.R., DIETRICH, W.E. A physically based model for the topographic control on shallow landsliding. Water Resour Res, 30, p. 1153–1171, 1994.

MURPHY, B.; VAZE, J.; TENG, J.; TUTEJA, N.K.; GALLANT, J.; SUMMERELL, G.; YOUNG, J. e WILD, J., Modelling landscapes using terrain analysis to delineate landforms and predict soil depths – examples from catchments in NSW. MODSIM, 2005.

NEMČOK, A., PAŠEK, J., RYBÁŘ, J. Classification of landslides and other mass movements. *Rock mechanics*, 4, p. 71-78, 1972.

PELLETIER, J.D., MALAMUD, B.D., BLODGETT, T., TURCOTTE, D.L., Scale-invariance of soil moisture variability and its implications for the frequency-size distribution of landslides. *Engineering Geology*, 48, p. 255-268, 1997.

REMONDO, J., GONZÁLES-DÍEZ, A., DE TERÁN, J.R.D., CENDERERO, A. Landslide Susceptibility Models Utilising Spatial Data Analysis Techniques. A Case Study from the Lower Deba Valley, Guipuzcoa (Spain). *Natural Hazards*, 30, p. 267-279, 2003.

ROCHA, E. M., Custos humanos e econômicos gerados por desastres naturais ocorridos no Brasil nos últimos 25 anos. In: Simpósio brasileiro de desastres naturais, 2004, Florianópolis. *Anais do Simpósio brasileiro de desastres naturais*. Florianópolis, 2004. p. 485-498.

SAFAEI, M., OMAR, H., HUAT, B.K., YOUSOF, Z.B.M., GHIASI, V. Deterministic Rainfall Induced Landslide Approaches, Advantage and Limitation. *Electron J Geotech Eng.*, 16, 1619-1650, 2011.

SCHWARZ, M., COHEN, D., OR, D. Root-soil mechanical interactions during pullout and failure of root bundles, *J. Geophysics*, 115, 2010.

SIDLE, R. C., PEARCE, A. J., O'LOUGHLIN, C. L. Hillslope stability and land use, *Water Resources Monograph Series*, Washington. 1985.

SIDLE, R.C, OCHIAI, H. Landslides: Process, Prediction, and Land Use. American Geophysical Union. Washington, 2000.

PACK, R.T., TARBOTON, D.G., GOODWIN, C.N. Terrain Stability Mapping with SINMAP, technical description and users guide for version 1.00. Terratech Consulting Ltd., Salmon Arm, B.C., Canada, 1998.

TABALIIPA, N.L.; FIORI, A.P. Influência da vegetação na estabilidade de taludes na bacia do rio Ligeiro (PR). *GEOCIÊNCIAS*, V. 27, N. 3, P. 387-399, UNESP, 2008.

TENG, J.; VAZE, J.; TUTEJA, N.K; GALLANT, J.C. A GIS-Based Tool for Spatial and Distributed Hydrological Modelling: CLASS Spatial Analyst. *Transactions in GIS*, 12, 2, p. 209-225, 2008.

VANHONI, F., MENDONÇA, F. O Clima Do Litoral Do Estado Do Paraná. *Revista Brasileira de Climatologia*, 3, p. 49-63, 2008.

VIEIRA, B. C. and FERNANDES, N. F. Landslides in Rio de Janeiro: the role played by variations in soil hydraulic conductivity. *Hydrological Processes*, 18, p. 791-805, 2004.

VIEIRA, B.C., Caracterização in situ da condutividade hidráulica dos solos e sua influência no condicionamento dos deslizamentos da bacia do rio Papagaio, maciço da Tijuca (RJ). 2001. Master thesis (Master in Geography) UFRJ, Rio de Janeiro.

VIEIRA, B.C. Previsão de escorregamentos translacionais rasos na Serra do Mar (SP) a partir de modelos matemáticos em bases físicas. 2007. Doctoral thesis (Doctorate in Geography). UFRJ, Rio de Janeiro.

WANG, G.; SASSA, K. Pore-Pressure Generation And Movement Of Rainfall-Induced Landslides: Effects Of Grain Size-Particle Content. *Engineering Geology*, 69, p. 109-125, 2003.

WESTEN, C.J.; ASCJ, T.W.J.; SOETERS, R. Landslide hazard and risk zonation — why is it still so difficult? *Bulletin of engineering geology and the environment*, 65, p. 167-184, 2006.

WU, W., SIDLE, R.C. A Distributed Slope Stability Model for Steep Forested Basins Water Resources Research, 31, 2097–2110, 1995.

Recebido em: 12/05/2020.

Aprovado para publicação em: 28/04/2021.